Quantum Electronics **37** (7) 679–684 (2007)

PACS numbers: 02.90.+p; 42.55.–f
DOI: 10.1070/QE2007v037n07ABEH013493

Methods of computational physics in the problem of mathematical interpretation of laser investigations

M.S. Brodyn, V.N. Starkov

***Abstract*. It is shown that in laser experiments performed by using an 'imperfect' setup when instrumental distortions are considerable, sufficiently accurate results can be obtained by the modern methods of computational physics. It is found for the first time that a new instrumental function – the 'cap' function – a 'sister' of a Gaussian curve proved to be demanded namely in laser experiments. A new mathematical model of a measurement path and carefully performed computational experiment show that a light beam transmitted through a mesoporous film has actually a narrower intensity distribution than the detected beam, and the amplitude of the real intensity distribution is twice as large as that for measured intensity distributions.**

Keywords: *computational physics, interpretation, laser, mathematical model, nanofilm, experiment.*

There exists the concept of the reduction to an ideal instrument in the scientific literature [1]. The ultimate possibilities of experimental setups are caused by physical phenomena forming the measurement process. A mathematical model of phenomena controlling the measurement process can be used to attempt to compensate their distorting action on the measurement data. The result of such mathematical transformation is treated as data obtained by using a virtual setup with possibilities exceeding considerably those of a real setup. One of the aims of laser experimental studies is to obtain the real intensity distribution which is not distorted by the measurement process. This goal can be achieved by various methods, for example, by using perfect instruments with the half-width of the instrumental function much narrower than the details of the intensity distribution under study. Another approach is the use of mathematical methods. In many cases, when instrumental distortions are considerable, the mathematical problem is reduced to the determination of the function $\upsilon(x)$ from the known instrumental function $K(x, y)$ and detected function $u(x)$, i.e., in particular, to the solution of the linear integral Fredholm equation of the first kind. The required function $\upsilon(x)$, determined mathematically, can be interpreted as the result of measurements on a model (virtual) setup with parameters exceeding the ultimate parameters of the equipment used.

M.S. Brodyn, V.N. Starkov Institute of Physics, National Academy of Sciences of Ukraine, prosp. Nauki 46, 03028 Kiev, Ukraine;
e-mail: sergeyyakunin@ukr.net

Received 13 December 2006
Kvantovaya Elektronika **37** (7) 679–684 (2007)
Translated by M.N. Sapozhnikov

The aim of this paper is to show by the example of specific laser experiments that the methods of computational physics allow an experimenter to obtain in some cases sufficiently accurate results by using an 'imperfect' setup.

We solve the problem of mathematical interpretation of the results of experimental studies of the optical properties of thin layers of porous materials (in particular, silicon dioxide SiO_2 and titanium dioxide TiO_2). Recently, interest was aroused in the study of thin nanocrystal films because they can be potentially used in photovoltaic systems, sensor devices, photocatalysis, microelectronics, operative memory devices in computers, etc. These materials have a high refractive index, high strength and long-term stable optical properties, and are transparent in the visible region. The methods developed at present provide the manufacturing of low-cost and high-quality films with the specified parameters.

The linear optical parameters of films include the dispersion dependences of the refractive index and absorption coefficient as well as the spatial distribution of the scattering intensity. The linear parameters are used as the initial data to analyse nonlinearity; however, they are themselves also of interest.

Scattering is studied first of all to measure correctly absorption in a film, i.e. to take into account the contribution of the integrated scattering intensity to the total decrease in the laser-beam power transmitted through the film. In addition, the details of the spatial intensity distribution of scattering contain information on the film structure, including the roughness of its surface, the size of clusters of nanoparticles forming the film, etc.

In experiments, the scattering indicatrix of mesoporous films was measured. One of the aims of measurements was to obtain the real scattering intensity distribution, i.e. the distribution not distorted by the instrument. The quintessence of the problem of mathematical interpretation of experimental results is that in most of the physical studies the required element υ characterising a physical object or phenomenon under study cannot be directly observed, and for this reason some of its manifestations is investigated, which can be represented in the form [2]

$$u = A\upsilon, \quad A : V \to U, \quad \upsilon \in V, \quad u \in U,$$

where A is a linear and compact operator acting from the Hilbert space V to the Hilbert space U, i.e. an experimenter fixes an image u of the real element υ of the state of the object, phenomenon or process.

The solution of the problem of reconstructing the element υ involves two main stages:

(i) The construction of the operator A acting on the element υ ($\upsilon \in V, u \in U,\ A : V \to U$);

(ii) the determination of the characteristics of the model of element υ from the known element u and operator A, i.e. the solution of the operator equation $u = A\upsilon$ ($\upsilon \in V, u \in U$).

The construction of the operator A is called the stage of modelling the measurement path of the experimental setup because it distorts the element υ. This operator can be often represented in the form

$$A\upsilon \equiv \int_c^d K(x,s)\upsilon(s)\mathrm{d}s, \tag{1}$$

where $\upsilon(s)$ is the required function; $c \leqslant s \leqslant d$; and $K(x,s)$ is the instrumental function satisfying the relations

$$\int_c^d K(x,s)\upsilon(s)\,\mathrm{d}s = u(x), \quad a \leqslant x \leqslant b, \tag{2}$$

$$K(x,s) \in C([a,b] \times [c,d]), u \in L_2(a,b).$$

In physical studies, the instrumental function is a characteristic of a linear measurement device which relates the measured quantity at the device output to the real value of this quantity at the device input. The problem upon this approach involves the determination of the function $\upsilon(s)$ from the known instrumental $[K(x,s)]$ and detected $[u(x)]$ functions, i.e. the solution of the linear Fredholm equation of the first kind, which has in the general case the form

$$u(x) = \int_c^d K(x,s)\,\upsilon(s)\mathrm{d}s. \tag{3}$$

The scheme of the experiment is presented in Fig. 1 [3]. The diameter of the polarised Gaussian 632.8-nm, 1-mW beam from a He–Ne laser was ~ 0.95 mm in the sample plane. The sample mounted on the goniometer axis (perpendicular to the laser beam) was a thin (~ 1 μm) film of a porous material deposited on a glass substrate. Scattered light was collected with a lens mounted on the movable arm of the goniometer. Behind the lens, a CCD camera was mounted at a distance of 8.6 cm from a sample. In the lens plane, an opaque screen was placed which has a hole of diameter equal to that of the lens (1 cm). We measured the meridional angular dependence (the rotation axis of a photodetector lies in the sample plane) of the scattered light intensity with respect to the propagation direction of the laser beam perpendicular to the porous film. The scattering intensity was measured for each position of the lens with the photodetector by summing intensities on all elements of the CCD array.

The mathematic interpretation of the experimental results assumes first of all the acquisition of information on a virtual setup with parameters exceeding the ultimate parameters of the experimental equipment. Therefore, the solution of the problem of increasing the informational reliability of experimental data being detected begins with the construction of a mathematical model of the experimental setup.

When the results of experiments are analysed, the question appears about the relation between the intensity of light scattered in front of a lens and the intensity recorded with a CCD camera. This problem can be solved in the following way.

The infinitesimal value of the detected intensity is approximately determined by the expression

$$\Delta u = \upsilon G \Delta S,$$

where υ is the real scattering intensity; G is the radiation transmission function of the lens at the point of laser beam incidence; ΔS is the element of the circle area occupied by the lens (Fig. 2). The expression for the radiation intensity measured by the CCD camera can be written in this case in the form

$$u(x) = \iint_S \upsilon\, G\, \mathrm{d}s\, \mathrm{d}t,\ \ x \in [-a_0, a_0], \tag{4}$$

where x is the coordinate of the lens centre.

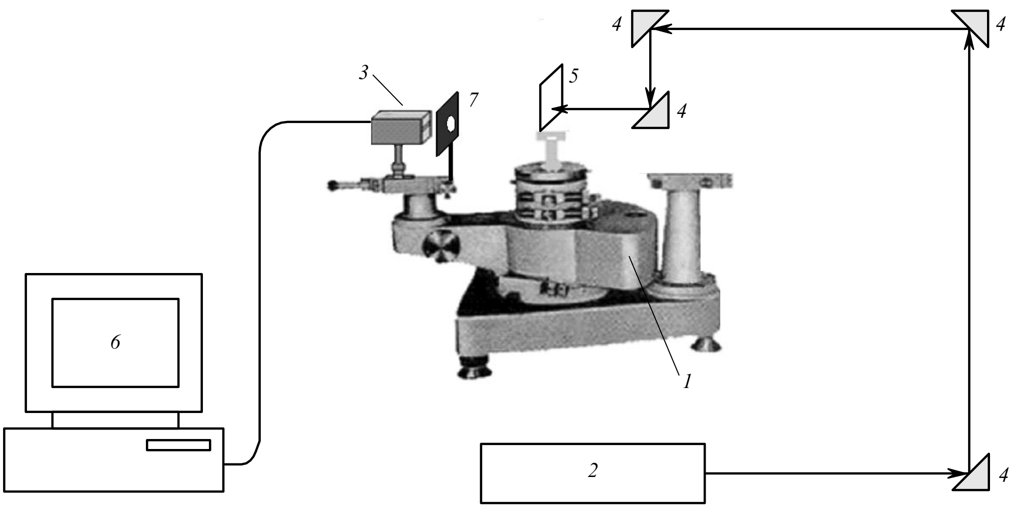

Figure 1. Scheme of the experimental setup for measuring the spatial distribution of the light intensity: (*1*) G-5 goniometer; (*2*) He–Ne laser; (*3*) photodiode array; (*4*) set of deflecting prisms; (*5*) sample; (*6*) computer; (*7*) screen with a lens.

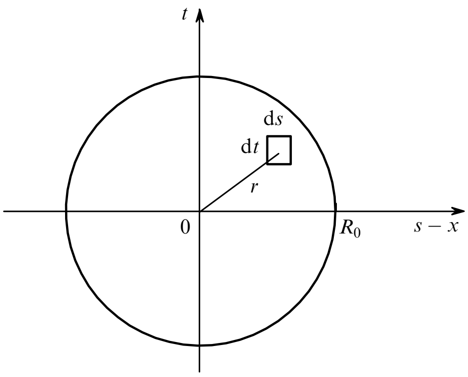

Figure 2. To the calculation of the scattered radiation intensity recorded with a CCD camera.

Let us make several remarks concerning the functions υ and G. In the general case, υ is a function of the two variables s and t. However, because it is the prototype of the function of one variable $u(x)$ in mapping (4), we can treat it also as the function of one variable $\upsilon(s)$. It is also reasonable to assume that the function G is axially symmetric and depends only on the radius $r \in [0, R_0]$, , where R_0 is the lens radius. Taking these remarks into account, expression (4) can be written in the form

$$u(x) = \int_{x-R_0}^{x+R_0} \int_{-[R_0^2-(x-s)^2]^{1/2}}^{[R_0^2-(x-s)^2]^{1/2}} \upsilon(s) G(r) \mathrm{d}s\, \mathrm{d}t. \qquad (5)$$

By using the radius r as the integration variable, we obtain

$$u(x) = \int_{x-R_0}^{x+R_0} \upsilon(s)\mathrm{d}s \int_0^{R_0} G(r)$$

$$\times \frac{2r}{[r^2-(x-s)^2]^{1/2}} \mathrm{d}r, \quad |x-s| \leqslant r, \qquad (6)$$

or

$$u(x) = \int_{-R_0}^{R_0} K(s)\upsilon(x-s)\mathrm{d}s, \quad x \in [-a_0, a_0], \qquad (7)$$

where

$$K(s) = \int_{|s|}^{R_0} G(r) \frac{2r}{(r^2-s^2)^{1/2}} \mathrm{d}r. \qquad (8)$$

Relations (7) and (8) should be supplemented with an *a priori* physical condition

$$\upsilon(s) \geqslant 0, \quad \forall\, s \in (-\infty, \infty). \qquad (9)$$

It should be emphasised that the solution of problem (7), (9) involves serious difficulties related to measurements errors. It was assumed so far that the instrumental function $K(s)$ and detected function $u(s)$ required for determining the required function $\upsilon(s)$ are known exactly. However, both these function can be actually determined only by measuring experimentally $u(x)$ and $G(r)$ with a CCD camera. These measurements always have errors related to the properties and errors of the measurement path (defects of the optics of the instrument, its focusing, etc.).

It follows from (8) that the function $K(s)$ can be in fact determined from the known experimental values of the transmission function $G(r)$.

The dependence $G(r)$ was measured on the setup described above in the absence of a sample, i.e. a laser beam scanned the lens along its diameter. The experimental values of $G(r)$ are presented in Fig. 3 [3]. The experimental dependence $\tilde{K}(s)$ can be found from these values by integrating (8). The experimental values of the instrumental function $\tilde{K}(s)$ are approximated by the 'cap' function [2, 4]

$$\hat{K}(s) = \theta(R^2 - s^2) C \exp\left(-\frac{R^2}{R^2 - s^2}\right), \quad -R \leqslant s \leqslant R, \quad (10)$$

where $\theta(R^2 - s^2)$ is the Heaviside function; $C = 4.13$ cm^{-1}; and $R = 0.545$ cm. Figure 4 presents the best fit of the values of $\hat{K}(s)$ by the function $\tilde{K}(s)$ in the metric $L_2(-R, R)$.

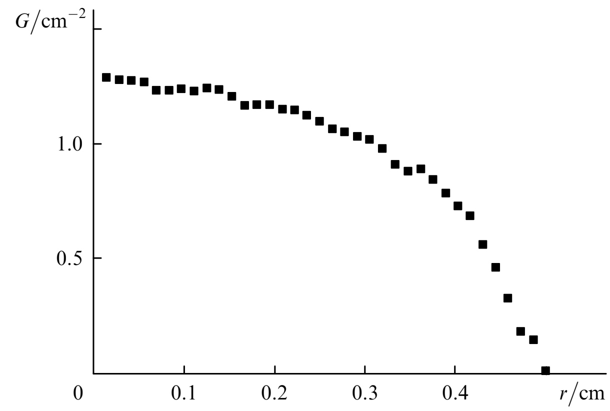

Figure 3. Experimental values of the function $G(r)$.

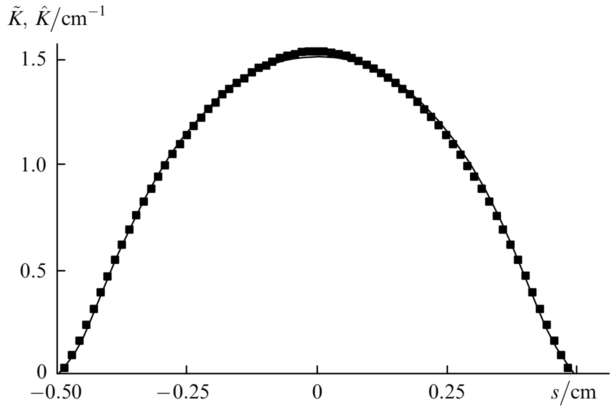

Figure 4. Experimental [$\tilde{K}(s)$, squares] and theoretical [$\hat{K}(s)$, solid curve] instrumental functions.

The instrumental 'cap' function is of great interest for practical applications because it has important properties. First, the error of approximation of the instrumental function by the 'cap' function is small: $\|\tilde{K}(s) - \hat{K}(s)\|_2 = 0.0157876$ (Fig. 4). Second this function is finite by definition, i.e. $\hat{K}(s) = 0$ for $|s| \geqslant R$. Third, it is infinitely differentiable with respect to s.

Due to its finiteness and infinite differentiability, the instrumental 'cap' function $\hat{K}(s)$ fundamentally differs from the instrumental functions well-known in physics [2]. The set of instrumental functions including the diffraction function

$$K(x) = \frac{1}{\gamma}\left[\frac{\sin(\pi x/\gamma)}{\pi x/\gamma}\right]^2 \qquad (11)$$

(the half-width of the instrumental contour is determined by the relation $a = 0.886\gamma$), the slit function

$$K(x) = \begin{cases} 1/a & \text{при } |x|/a \leqslant 1/2, \\ 0 & \text{при } |x|/a > 1/2 \end{cases} \qquad (12)$$

(a is the slit image width), the Gaussian function

$$K(x) = \frac{2}{a}\left(\frac{\ln 2}{\pi}\right)^{1/2} \exp\left(-4\frac{x^2}{a^2}\ln 2\right), \qquad (13)$$

the dispersion function

$$K(x) = \frac{a/(2\pi)}{x^2 + (a/2)^2}, \qquad (14)$$

the Dirichlet function

$$K(x) = \frac{\sin(x/a)}{\pi x}, \qquad (15)$$

the exponential function

$$K(x) = \frac{\ln 2}{a}\exp\left(-2\frac{|x|}{a}\ln 2\right), \qquad (16)$$

and the triangular function

$$K(x) = \begin{cases} a^{-1}(1 - |x|/a) & \text{for } |x|/a \leqslant 1, \\ 0 & \text{for } |x|/a > 1, \end{cases} \qquad (17)$$

forms the subset of delta-like sequences (pulsed functions). Note, for example, that unlike the 'cap' function, the slit (12) and triangular (17) instrumental functions are finite, but have no continuous first derivatives. On the other hand, the Gaussian (11) and diffraction (11) instrumental functions are infinitely differentiable, but not finite.

For comparison, Figure 5 presents the best fit of the instrumental function $\tilde{K}(s)$ by the Gaussian function $K_G(s)$. It is obvious that the 'cap' function $\hat{K}(s)$ much better approximates the experimental instrumental function because

$$||\tilde{K}(s) - K_G(s)||_2 = 0.135952,$$

$$K_G(s) = 1.639\exp(-7.56066 s^2).$$

By returning to the reduction problem, we consider the methods used for solving integral equation (7) (the convolution equation) when the recorded function $u(x)$ and the instrumental function $K(s)$ are known.

It should be emphasised that the specific feature of inverse problems (3) and (7) is that the observed function $u(x)$ is an integral and, therefore, it is weakly sensitive to large variations in the function $v(s)$ when these variations compensate each other. This means that two substantially different functions $v(s)$ may correspond to close experimen-

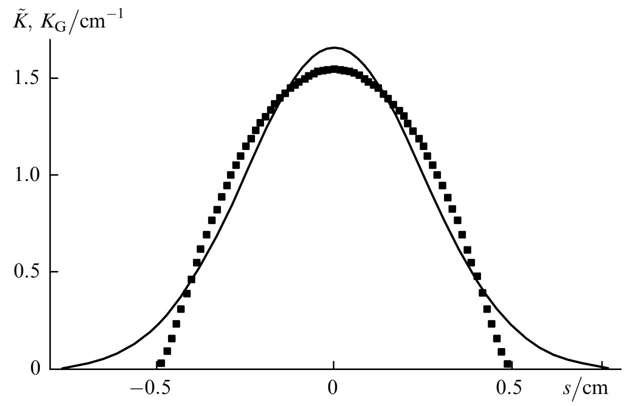

Figure 5. Experimental [$\tilde{K}(s)$, squares] and theoretical [$K_G(s)$, solid curve] instrumental functions.

tal functions. Because experimental functions are always measured with some error, the problem of determining the approximate solution of the inverse problem (7) close to the real solution appears. It is this problem that is basic from the mathematical point of view for the interpretation of experimental results.

It is known that the solution of Eqn (7) exists and is unique if the Fourier transform of the instrumental function does not vanish in any finite interval.

The classical method for solving convolution equations with the help of the direct and inverse Fourier transforms is as follows. Let $u(x) \in L_2(-\infty, \infty)$, $K(s) \in L_1(-\infty, \infty)$, and $v(s) \in L_1(-\infty, \infty)$, then the solution of Eqn (7) is determined by the expression

$$v(s) = \frac{1}{2\pi}\int_{-\infty}^{\infty} \frac{U(\omega)}{K(\omega)}\exp(-\mathrm{i}s\omega)\mathrm{d}\omega, \; s \in (-\infty, \infty), \qquad (18)$$

where $U(\omega)$ and $K(\omega)$ are the Fourier transforms of the observed function $u(x)$ and the instrumental function $K(s)$, i.e.

$$U(\omega) = \int_{-\infty}^{\infty} u(x)\exp(\mathrm{i}\omega x)\mathrm{d}x,$$

$$K(\omega) = \int_{-\infty}^{\infty} K(s)\exp(\mathrm{i}\omega s)\mathrm{d}s.$$

If for $\omega \to \infty$ the Fourier transforms $U(\omega)$ and $K(\omega)$ tend consistently to zero, so that

$$\lim_{\omega\to\infty}[U(\omega)/K(\omega)] = 0,$$

and integral (11) converges, then the solution $v(s)$ exists, is unique and described by expression (18), i.e. for exact $u(x)$ and $K(s)$, the first two points of the Hadamard definition of the problem correctness can be fulfilled.

However, the use of expression (18) involved difficulties already at this stage because the operation with infinite limits is possible only in the case when the functions $U(\omega)$ and $K(\omega)$ are represented analytically. The analytic expression for the Fourier transform of the instrumental function in the form of a 'cap' is absent.

As mentioned above, serious problems appear due to the errors in measurements of intensity distributions, which are related to the properties and errors of the measurement path. In the presence of measurement errors, the resulting contour can be represented in the form

$$\tilde{u}(x) = u(x) + \delta(x),$$

where $\delta(x)$ is the 'noise' containing, in particular, the white noise component. As a result, the function $\tilde{U}(\omega)$ tends not to zero when $\omega \to \infty$ but to a constant depending on the white noise level. Then,

$$\lim_{\omega \to \infty} [\tilde{U}(\omega)/K(\omega)] = \infty$$

and, as follows from (18), Eqn (4) has no solution. Thus, the high harmonics in the solution $v(s)$ are sensitive even to small errors in the determination of $u(x)$. This means that the neglect of the instability of the problem of reduction to the ideal instrument can lead to the erroneous interpretation of experimental measurements.

As mentioned above, the Fourier transform of the 'cap' function $\hat{K}(s)$ has no the analytic representation. Figure 6 presents the spectrum $\hat{K}(\omega)$ calculated numerically. It follows from this calculation that the instrumental 'cap' function $\hat{K}(s)$ has a property which strongly complicates the solution of the initial problem: namely, the Fourier transform of the 'cap' has the denumerable set of zeroes.

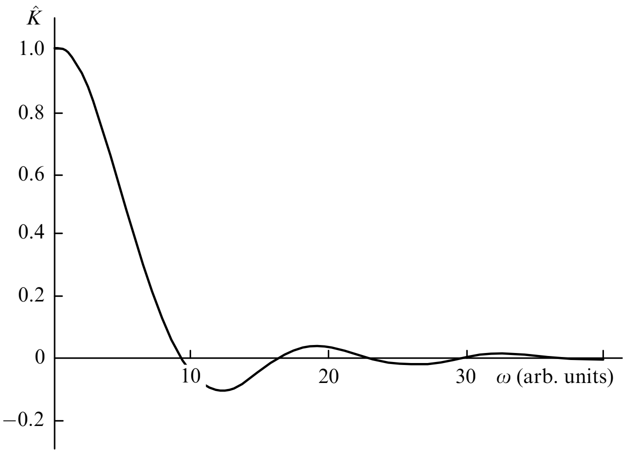

Figure 6. Fourier transform of the 'cap' function $\hat{K}(\omega)$.

Taking into account the reasons listed above, the solution of the integral convolution equation (7) is a substantially ill-posed problem. One of the most efficient methods for approximating solving ill-posed problems is the iterative Landweber method [5]. The integral equation (7) can be solved, taking condition (9) into account, by using the spline-iterative modification of the Landweber method developed in [6]:

$$v_0(s) = 0, \ s \in [-\alpha, \alpha], \ \ v_m(s) = v^{\mathrm{G}}_{m-1}(s)$$

$$+ \eta[F(s) - \int_{-\alpha}^{\alpha} \Re(s,t) \, v^{\mathrm{G}}_{m-1}(t)\mathrm{d}t], \ m = 1, 2, \ldots,$$

$$v^{\mathrm{G}}_m(s) = g_m \exp(-s^2/h_m^2)$$

$$= \arg \min_{g \geqslant 0, h>0} ||v_m(s) - g\exp(-s^2/h^2)||,$$

$$0 < \eta < 2/||A^*A||, \quad F(s) = \int_{-a_0}^{a_0} \hat{K}(x,s)\tilde{u}(x)\mathrm{d}x,$$

$$\alpha = a_0 + R, \quad \Re(t,s) = \Re(s,t) = \int_{-a_0}^{a_0} \hat{K}(x,t)\hat{K}(x,s)\mathrm{d}x,$$

$$||A^*A||^2 = ||\Re(t,s)||^2 \leqslant \int_{-\alpha}^{\alpha}\int_{-\alpha}^{\alpha} \Re^2(t,s)\mathrm{d}t\,\mathrm{d}s.$$

The condition for the going out of the iterative cycle is that the norm of the difference of the adjacent solutions should not exceed 10^{-8} after the stabilisation of the values of g_m and h_m up to six significant digits inclusive. The number of iterations m satisfying these requirements in the numerical experiment considered above was 375. As the observed function $\tilde{u}(x)$, the interpolation cubic spline of detected experimental data was used (Fig. 7) [6, 7].

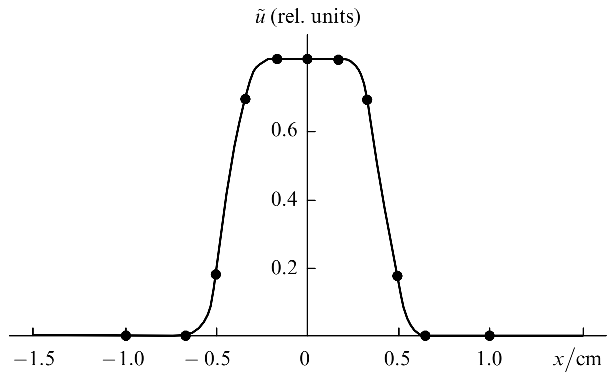

Figure 7. Experimental function $\tilde{u}(x)$ (circles) and its interpolation cubic spline (solid curve).

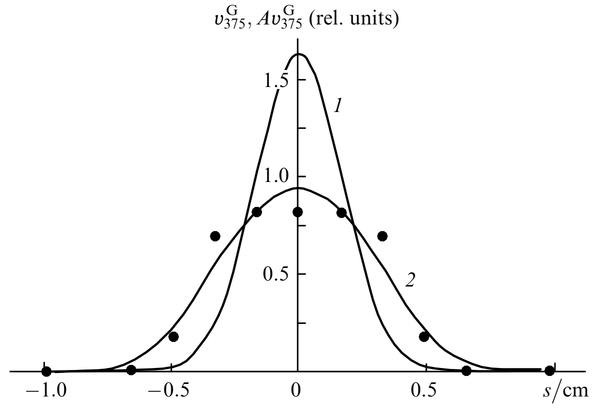

Figure 8. Distributions of the real scattering intensity $v^{\mathrm{G}}_{375} = 1.62725\exp(-17.2906\,s^2)$ (*1*) and its Fourier transform Av^{G}_{375} (*2*). Circles are experimental data.

Fig. 8 presents the results of the numerical experiment: the real scattering intensity $v^{\mathrm{G}}_{375}(s) = 1.62725\exp(-17.2906 \times s^2)$, its Fourier transform $Av^{\mathrm{G}}_{375}(s)$, and experimental data. In this case, the residual was

$$||Av^{\mathrm{G}}_{375} - \tilde{u}||_2^2 = 0.0110802.$$

In conclusion, we present the main results of the paper:

(i) The mathematical model has been constructed in the form of the integral Fredholm equation of the first kind for the first measurement path of the experimental laser setup for studying the optical properties of porous nanofilms;

(ii) the use of the 'cap' function

$$\hat{K}(s) = \theta(R^2 - s^2) C \exp[-R^2/(R^2 - s^2)],$$

[where $\theta(R^2 - s^2)$ is the Heaviside function] has been substantiated in the addition to the known instrumental functions;

(iii) the theory of spline-iterative methods of computational physics has been developed and the spline-iterative modification of the Landweber method for solving the integral Fredholm equation of the first kind has been elaborated;

(iv) it has been found in numerical experiments that the mathematical interpretation corrects the results of laser measurements, and the amplitude of the real intensity distribution is twice as large as that of measured distributions;

(v) the mathematical interpretation of experimental results has shown that a light beam transmitted through a mesoporous film has a narrower intensity distribution than the recorded beam.

References

1. Rautian SG. *Usp. Fiz. Nauk*, **66**, 475 (1958).
2. Starkov V.N. *Konstruktivnye metody vychislitel'noi fiziki v zadachakh interpretatsii* (Constructive Methods of Computational Physics in Interpretation Problems) (Kiev: Naukova Dumka, 2002).
3. Borshch A.O., Brodyn M.S., Gayvoronsky V.Ya., Maksyutenko P.V., Starkov V.N. *Ukr. J. Phys.*, **49**, 196 (2004).
4. Starkov V.N. *Probl. Upr. Inform.*, (5), 97 (2001).
5. Landweber L. *Amer. J. Math.*, **73**, 615 (1951).
6. Starkov V.N. *Trudy Mezhdunarodn. konf. 'Tikhonov i sovremennaya matematika'. Obratnye i nekorrektno postavlennye zadachi* (Proceedings of the International Conference 'Tikhonov and Modern Mathematics'. The inverse and Ill-posed Problems) (Moscow: Moscow State University, 2006).
7. Borshch A.A., Brodyn M.S., Gayvoronsky V.Ya, Starkov V.N., Yakunin S.V., in *Pitannya optimizatsii obchislen'* (Study of the Optimisation of Calculations) (Kiev: V.M. Gluskov Institute of Cybernetics, NAS, Ukraine, 2005).